Inner Shell Ionizations by Proton Impact*

J. D. Garcia

Physics Department, University of Arizona, Tucson, Arizona 85721

NGR-03-002-017

Abstract

Cross sections for production of inner shell vacancies in atoms by proton impact have been examined in an impulse approximation. The model used includes modifications to account for the nuclear repulsion of the proton. Comparisons with experiment and with other calculations are made. It is found that the model compares favorably with existing Born approximations. If the most recent fluorescent yield data are used, the present results agree well with experiment for proton energies larger than ~ 300 times the electron binding energies. Determination of fluorescent yields by means of such experiments is also discussed.

I. INTRODUCTION

Inner shell ionizations by proton impact have received considerable attention, both theoretical[1,2] and experimental.[3,4] The purpose of this note is primarily to indicate that the basic features of the process can be quantitatively understood using a very simple model.

A brief description of the model is presented in Section II, and comparisons with existing theory and with experiment are discussed in Section III. Determination of fluorescent yields is discussed in Section IV. The present results compare favorably at high energies with Born approximation results, and with the corrected values introduced by Bang and Hansteen[2] at lower energies. Comparison with experimental results indicates good agreement at higher energies.

II. IMPULSE OR BINARY ENCOUNTER MODEL

We assume that the dominant interaction producing the inner shell ionization is a direct energy exchange between the proton and the atomic electron in question. Since the classical and quantum mechanical center-of-mass differential cross sections for coulomb scattering are identical, we can utilize a classical analysis of the transformation to the laboratory frame, thus obtaining a differential cross section $d\sigma/d\Delta E$ for an exchange of energy ΔE between two charged particles. We then integrate over all energy exchanges from the binding energy of the electron to the total energy of the proton, and average over the velocity distribution of the bound electron. These considerations imply a strict conservation of energy and momentum in the electron-proton interaction. An approximate correction for the effect of the nuclear repulsion of the proton is also included.

A classical binary encounter approach including the motion of the bound electron was first proposed by Gryzinski.[5] It has been applied to total ionization by proton impact,[6] and reasonable agreement with experiment was obtained. For inner shell ionization, it is expected that agreement with experiment should be much better since the requisite energy exchange is quite large, making it less likely that other interactions contribute significantly to the process.

The cross section for the (laboratory frame) exchange of an energy ΔE between the incident proton whose velocity is $\vec{v}_1$, and an electron whose velocity is $\vec{v}_2$, averaged over a spherically symmetric distribution of directions for $\vec{v}_2$ has been given by Gerjuoy[7] and is easily integrated to give

$$\int_{\cdot}^{\Delta E} \frac{d\sigma}{d\Delta E}\, d\Delta E = \frac{\pi}{3}\,\frac{e^4}{v_1^2 v_2}\left[-\frac{2v_2^3}{(\Delta E)^2} - \frac{\frac{6v_2}{m_e}}{\Delta E}\right], \qquad 0 < \Delta E < b$$

$$= \frac{\pi}{3}\,\frac{e^2}{v_1^2 v_2}\left[3\,\frac{\frac{v_1}{m_1} - \frac{v_2}{m_2}}{\Delta E} + \frac{(v_2'^3 - v_2^3) - (v_1^3 + v_1'^3)}{(\Delta E)^2}\right] \qquad b < \Delta E < a$$

$$= \frac{\pi}{3}\,\frac{e^2}{v_1^2 v_2}\left[-\frac{2v_1'^3}{(\Delta E)^2}\right] \qquad \Delta E > a \text{ and } 2m_e v_2 > (m_1 - m_e)v_1$$

$$= 0 \qquad \Delta E > a \text{ and } 2m_e v_2 < (m_1 - m_e)v_1 \qquad (1)$$

where

$$a = \frac{4m_1m_e}{(m_1+m_e)^2}\left[E_1 - E_2 + \frac{v_1v_2}{2}(m_1 - m_e)\right] \quad ,$$

$$b = \frac{4m_1m_e}{(m_1+m_e)^2}\left[E_1 - E_2 - \frac{v_1v_2}{2}(m_1 - m_e)\right] \quad ,$$

$$v_1' = \left(v_1^2 - \frac{2\Delta E}{m_1}\right)^{1/2} \quad , \quad v_2' = \left(v_2^2 + \frac{2\Delta E}{m_e}\right)^{1/2} \quad .$$

The cross section for removal of an electron whose binding energy is u and whose speed is v_2 is given by Eq. (1) with an upper limit E, and a lower limit u:

$$\sigma_i = \int_u^{E_1} \frac{d\sigma}{d\Delta E}\, d\Delta E$$

The final classical expression for the cross section follows from this upon averaging over the speed distribution of the bound electron, and summing over all electrons in the subshell:

$$\sigma_I^{(v_1)} = N_i \int_0^{\infty} \sigma_i(v_1, v_2)\, f(v_2)\, dv_2 \qquad (2)$$

where N_i is the number of equivalent electrons having binding energy u, and $f(v_2)$ is the speed distribution of these electrons.

Classically, the speed distributions can be obtained from a microcanonical ensemble, as is well known. Given that the electron is in a state of total energy = - u, we ask for the probability that it have

a velocity (we consider a hydrogenic atom for simplicity)

$$f(v_2) = c \int \delta(H - E)\, d^3r$$

$$= c \int_0^\infty \delta\left(\frac{mv_2^2}{2} - \frac{ze^2}{r} + u\right) 4\pi r^2 dr \qquad (3)$$

This results in a speed distribution, when normalized to one electron, given by

$$f(v_2) = \frac{32}{\pi} v_o^5 \cdot \frac{v_2^2}{(v_2^2 + v_o^2)^4} \qquad (4)$$

where $v_o = \frac{(2u)^{1/2}}{m}$. This is identical with the quantum mechanical result for hydrogenic states.

While Eq. (2) has been obtained by classical methods, the cross section thus predicted is identical with that which would be obtained using the impulse approximation and product wave functions for the atomic states.[8] This is true here because we are considering only electrons in a given subshell, so that the coulomb amplitudes for each electron in the impulse approximation (and neglecting the Pauli principle) are identical. The classical sum of the squares of the amplitudes then coincides, because of the coincidence of the elastic center-of-mass cross section, with the quantal result. The relation to the Born approximation has been discussed elsewhere.[9]

Approximate expressions have been obtained[10] for including the effect of nuclear repulsion on the motion of the proton. The essential notion can be seen in Fig. 1. If the energy exchange between the proton

and electron takes place at the point P, the impact parameters for no nuclear charge would be ρ, but since the proton is repelled, the true impact parameter is b. Further, the kinetic energy of the proton is reduced because of its motion in the repulsive field. These two effects are incorporated into the cross section by the expression[10] (assuming the repulsion to be due to a point charge z' at the origin)

$$\sigma_I(E_1) = \sigma_I(E_1') \left\{\frac{1}{2} + \frac{1}{2}\left[1 - \frac{2z'E^2}{E_1\sigma(E_1')}\left(\xi - \left(\xi^2 - \frac{\sigma(E_1')}{\pi}\right)^{1/2}\right)\right]^{-1/2}\right\}^2 \qquad (5)$$

where $\sigma_I(E_1')$ is the cross section (2) at an energy $E_1' = E_1 - \frac{z'e^2}{\xi}$. Expression (5) differs from the corresponding one in Ref. 10 (equation preceding Eq. 12) only by the sign of the z' term, as appropriate for positive particles incident. These corrections are expected to be very small for protons, except at very low energies.

We have used Eq. (5) with $\xi = r_A = \frac{ze^2}{2u}$ (the "radius" of the subshell whose binding energy is u) to approximate the effect of nuclear repulsion. (ξ should in fact be determined from some expression analogous to Eq. (6) of Ref. 10; however the correction due to this choice is unimportant). We note that with this choice of ξ, and for $\sigma_I < \pi r_A^2$. The expression (5) becomes

$$\sigma_I(E_1) \simeq \sigma_I(E_1') \left\{\frac{1}{2} + \frac{1}{2}\left[1 - \frac{2}{\pi}\,\frac{\frac{z'}{z}}{\frac{E_1}{u}}\right]^{1/2}\right\}^2 \qquad (6)$$

and $E_1' = E_1 - \frac{2z'}{z}u$. This reaffirms that proton trajectories are rather stiff: the maximum "bending" correction is a factor of 4, and in fact, the bracket term differs from unity by only a few percent at

energies which have been experimentally investigated. Most of the correction comes from the change in kinetic energy of the proton, which is important only near threshold. We have taken advantage of the fact that (at least for K-shells) $z' \to z$ for large z, and used $z' = z$ only.

III. COMPARISONS

A. K-Shell Ionization

We have compared the results of the above model, using the hydrogenic distribution (4) in (2) and the correction from (5), to experimentally determined K-shell ionization cross sections for C, O, Mg, and Aℓ in Figs. 2 through 5. (For K-shells, $N_i = 2$). Also shown are the Born approximation results, where available. In Fig. 4 the effect of the corrections in (5) is displayed; the crosses show the uncorrected value (2) and the solid line is that obtained from (5). The triangles in Fig. 4 show also the values obtained by Bang and Hansteen,[2] who approximate the effect of nuclear repulsion in the Born framework also.

In Fig. 2, two sets of experimental values are shown.[11] The solid circles indicate the data using $\omega_K = 0.007$, as assumed in Ref. 3. The open circles depict the same data, but using the fluorescence yield value from Ref. 12, $\omega_K = 0.0009$. The theoretical formula due to Wentzel reported in Ref. 12 (Eq. 26) yields a value $\omega_K = 0.00145$, intermediate between the two values shown. For Mg and Aℓ, the fluorescent yields used in Ref. 3 are within the range of experimental values given in Ref. 12 (which vary by nearly one order of magnitude) and are within a few percent of the theoretical value.

It can be seen from Fig. 4 that the corrections due to nuclear repulsions are small except at very low energies. In fact, from (5) we can see that the corrections are negligible for $E_1/u > 150$, are only 10% at $E_1/u = 50$, though they do decrease the cross section by a factor of 3 at $E/u = 10$. Not surprisingly, the impulse and Born approximations compare very favorably at higher energies. The present results agree well with the Bang and Hansteen model as shown in Fig. 4.

B. L- and M-Shell Ionization

For L- and M-shells, a speed distribution appropriate to these electrons is to be used in (2). However, these cross sections are not very sensitive to the velocity distributions used, at least for energies near and above the peak in the cross section ($E/u \sim 2000$). We have used (4) for calculating the L_{III}-shell ($N_i = 4$) and M_{IV}- and M_V-shell ($N_i = 4$ and 6, respectively) ionization cross sections shown in Figs. 6 and 7. Also shown in Fig. 5 is the Born approximation cross section from Ref. 13. For the Cu L_{III}-shell, the solid circles indicate the data as given in Ref. 4, where $\omega_L = 0.05$ was used. The open circles are the same data, adjusted to the value $\omega_L' = 0.0056$ as given in Ref. 12. The Ho fluorescent yield ω_L used in Ref. 3 is about 10% lower than that given in Ref. 12. Again, there is reasonable agreement with the Born values.

The agreement with the Bang and Hansteen calculations can be construed to mean that the effects of nuclear repulsion have been reasonably approximated. It is thus expected that a full distorted wave Born approximation would be in better agreement with the impulse

approximation and with experiment. However, it can be seen that these corrections do not suffice for energies $E/u \leq 100$. At these energies, the proton speed is much less than the average orbital electron speeds, and adiabatic energy changes become important.

IV. CONCLUSIONS

Though we have presented only a sample of comparisons, it seems apparent that a binary encounter model accounts adequately for the process of inner shell ionization by proton impact, at least for energies $E_1/u \geq 300$. This is especially evident when the most recent values for fluorescent yield are used. As has been previously discussed,[6] the present method has the advantage of a scaling law: given the cross section for the removal of one electron whose binding energy is u_a by a proton of energy E_1, the cross section for the removal of an electron whose energy is u_b is given by

$$\sigma(u_b, E_1^*) = \left(\frac{u_a}{u_b}\right)^2 \sigma(u_a, E_1) \tag{6}$$

where $E_1^* = (u_b/u_a) E_1$. To facilitate further comparisons, Table I shows the cross section per K-shell electron for Mg K-shell ionization (u = 1305 eV). The values in Column 1 are those using (4) in (2), and Column 2 shows the results using (5).

The evidence accumulated to date (primarily from outer shell ionizations) indicates that both Born and impulse approximations provide estimates of ionization cross sections which are reliable to within a factor of about 2, for proton energies $E_1/u \geq 300$. This statement is true

for outer shell ionizations; it is expected that an impulse approximation should be more applicable to inner shell ionizations, where the energy transfer is larger and is more likely to be the dominant process. At lower energies, these approximations describe the process much less adequately.

In the present case, the comparisons are somewhat hampered by uncertainties in the fluorescent yields, required to convert the experimental x-ray production cross sections into ionization cross sections. We can, however, utilize the above-mentioned reliability to establish a rule for an approximate determination of the fluorescent yield. This simply entails reversing the usual procedure and defining, for K-shell,

$$\omega_K = \frac{\sigma_x}{\sigma_I} \qquad \text{for } E_I/u \geq 1000 \qquad (7)$$

where σ_x is the x-ray production cross section and σ_I is the impulse approximation for the ionization cross section. The ω's so determined should be correct to within a factor of about 2.

On this basis (see Fig. 2), Eq. (7) predicts a value $\omega_K = 0.0018$ for carbon, which is only 25% different from the theoretical estimate and a factor of 2 from the value quoted in Ref. 12. Similarly, the values for Mg and Al would differ by only a few percent from the accepted values, as would that for the Cu L-shell. While the Ho L_{III}-shell data do not go high enough, the highest energy point yields a value $\omega_L = 0.29$, 30% higher than the value used in Ref. 3.

For M shells, we can adapt the suggestion in Ref. 12 (their Eq. (33)), to define

$$\omega_M = \frac{\sigma_x}{0.6\,\sigma_{M5} + 0.4\,\sigma_{M4}}$$

where σ_{M4}, σ_{M5} are the M IV and M V subshell ionization cross sections, respectively. This yields $\omega_M = 0.0028$ Gd and $\omega_M = 0.0052$ for Ho. These are less certain because the exact nature of the observed x-rays is unknown.

Both the uncertainties in the theory and in the experimental values prevent this method from being a very precise one at this time. However, it can be used to distinguish between values which differ by an order of magnitude as in the case of Al. The present results do confirm that the theoretical formula for K-shell fluorescent yields (Eq. (26) of Ref. 12) is quite reliable for low Z materials. For more accurate comparisons within this model it will be necessary to use velocity distributions in (2) determined by atomic wavefunctions better than the hydrogenic forms used here (e.g., Hartree-Fock).

Finally, it is apparent that measurements of proton x-ray production cross sections for very low-Z materials (Be, B, C) at proton energies sufficiently large to be well beyond the peak in the cross section (for example, at $E_1/u \sim 2$ or 3×10^4) would be very interesting. Such measurements have been done for H and He and verify the binary nature of the process for outer shell ionization (see Ref. 6). These measurements would provide a good test of this model for inner shell processes, as well as confirm the proposed fluorescent yield determination method.

ACKNOWLEDGMENTS

The author is grateful to the Lawrence Radiation Laboratory at Livermore, California, and to Dr. J. M. Khan for the hospitality extended him during the course of performing the work reported here.

Table I. Mg K-shell ionization cross section per electron.

Energy (keV)	σ_K/N_i Uncorrected	Corrected
20	4.6×10^{-25}	2.3×10^{-25}
30	2.3×10^{-24}	1.5×10^{-24}
40	6.5×10^{-24}	5.0×10^{-24}
60	2.5×10^{-23}	2.1×10^{-23}
80	6.0×10^{-23}	5.4×10^{-23}
100	1.2×10^{-22}	1.1×10^{-22}
200	8.6×10^{-22}	8.6×10^{-22}
400	4.3×10^{-21}	4.3×10^{-21}
600	8.8×10^{-21}	8.8×10^{-21}
800	1.3×10^{-20}	1.3×10^{-20}
1000	1.6×10^{-20}	1.6×10^{-20}
1500	2.3×10^{-20}	2.3×10^{-20}
2000	2.6×10^{-20}	2.6×10^{-20}
2800 (peak)	2.8×10^{-20}	2.8×10^{-20}
3000	2.7×10^{-20}	2.7×10^{-20}
4850	2.1×10^{-20}	2.1×10^{-20}

References

*Work supported in part by the U. S. AEC (LRL, Livermore, California) and in part by NASA and ONR (University of Arizona).

[1]E. Merzbacher and H. W. Lewis, Encyclopedia of Physics, ed. by S. Flugee. (Springer-Verlag, Berlin, 1958) V34, p. 166. See also W. Henneberg, Z. Physik 86, 592 (1933).

[2]J. Bang and J. M. Hansteen, Kgl. Danske Videnskab. Selskab., Mat. Fys. Medd., 31, No. 13 (1959).

[3]J. M. Khan, D. L. Potter, and R. D. Worley, Phys. Rev. 139, A1735 (1965).

[4]J. M. Khan, D. L. Potter, and R. D. Worley, Phys. Rev. 145, 23 (1966); R. R. Hart, F. W. Reuter III, H. P. Smith, Jr., and J. M. Khan, Phys. Rev. 179, 4 (1969).

[5]M. Gryzinski, Phys. Rev. 138, A336 (1965).

[6]J. D. Garcia, E. Gerjuoy, and J. E. Welker, Phys. Rev. 165, 66 (1968).

[7]E. Gerjuoy, Phys. Rev. 148, 54 (1966). Gryzinski (Ref. 5) also gives such a cross section, but uses various approximations and assumptions not all of which are justified. Equation (1) is exact.

[8]See N. F. Mott and H. S. W. Massey, The Theory of Atomic Collisions, (Oxford University Press, London, 1965), Chapter XII, Sec. 5, for a discussion of the impulse approximation.

[9]J. D. Garcia, Phys. Rev. 159, 39 (1967).

[10]B. K. Thomas and J. D. Garcia, Phys. Rev. 179, 94 (1969).

[11]The carbon data reported in Ref. 3 have been updated; the corrected values, aside from fluorescent yield values adopted, can be found in Phys. Rev. Letters 21, 1731 (1968). These latter values have been used in Fig. 2.

[12]R. W. Fink, R. C. Jopson, H. Mark and C. D. Swift, Rev. Mod. Phys. 38, 513 (1966).

[13]E. Merzbacher and J. S. Khandelwal, Phys. Rev. 151, 12 (1966).

Figure Captions

Fig. 1. Proton impact collision geometry.

Fig. 2. Carbon K-shell ionization by proton impact. Solid circles, experiment (Refs. 3, 10); open circles, corrected data; crossed circles, Born approximation (Ref. 3). Solid line, present results.

Fig. 3. Oxygen K-shell ionization by proton impact. Solid circles, experiment (Ref. 4); open circles, corrected data, using $\omega_L = 4.55 \times 10^{-3}$ from theory (Ref. 12); solid line, present results.

Fig. 4. Magnesium K-shell ionization by proton impact. Open circles, experiment (Ref. 3); crossed circles, Born approximation; solid line, present results; crosses, present results uncorrected for repulsion.

Fig. 5. Aluminum K-shell ionization by proton impact. Open circles, experiment (Ref. 3); crossed circles, Born approximation (Ref. 3); triangles, Bang and Hansteen model (Ref. 2); solid line, present results.

Fig. 6. L-shell ionization by proton impact. A. Holmium L III-subshell. Circles, experiment (Ref. 3); solid line, present results. B. Copper L III-subshell. Solid circles, experiment (Ref. 4); open circles, corrected data; crossed circles, Born approximation (Ref. 12); solid line, present results.

Fig. 7. M-shell ionization by proton impact. A. Holmium M-shell: open circles, experiment (Ref. 3); solid lines, present results. B. Gadolinium M-shell: open circles, experiment; solid lines, present results.

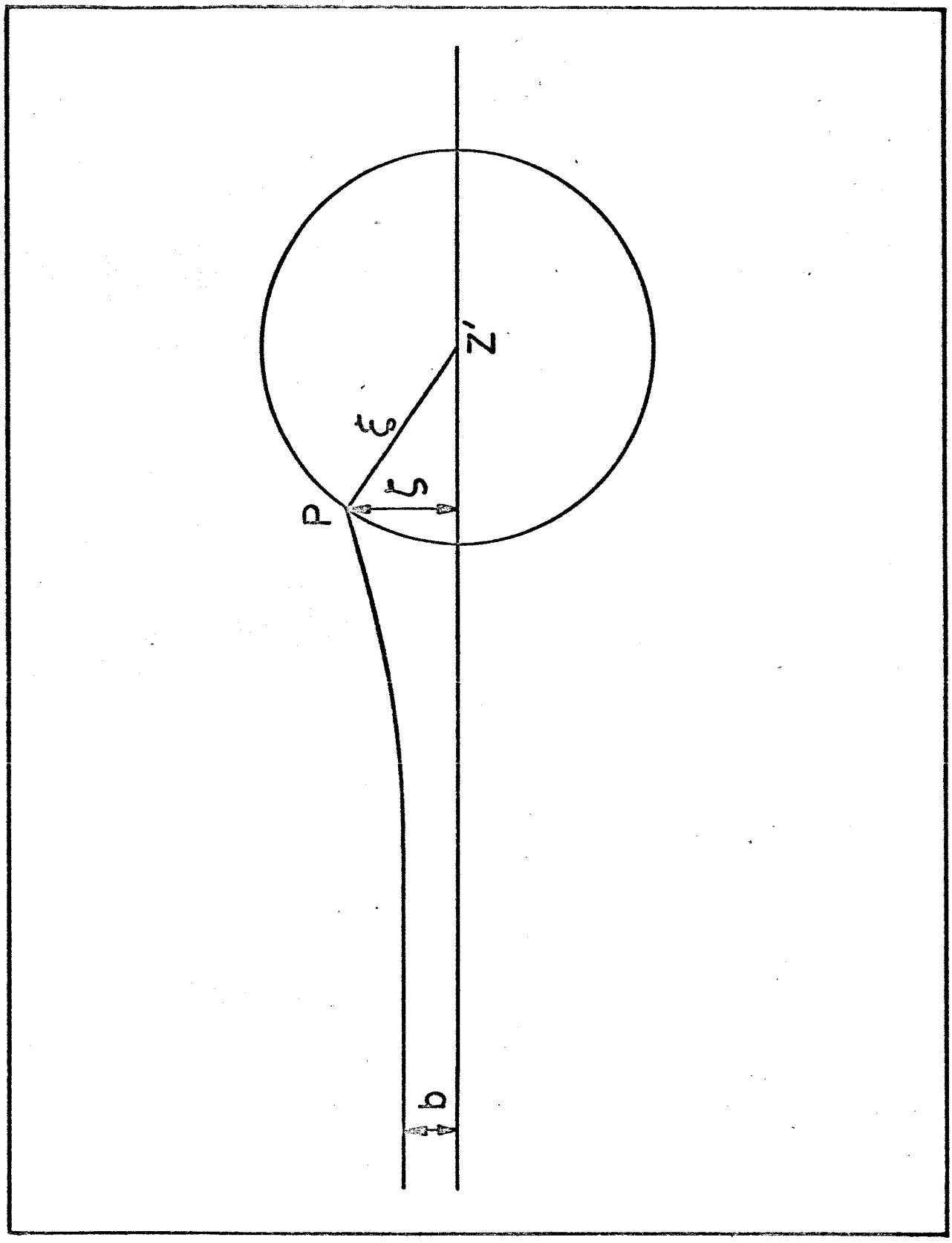
Z'
ε
ξ
P
b

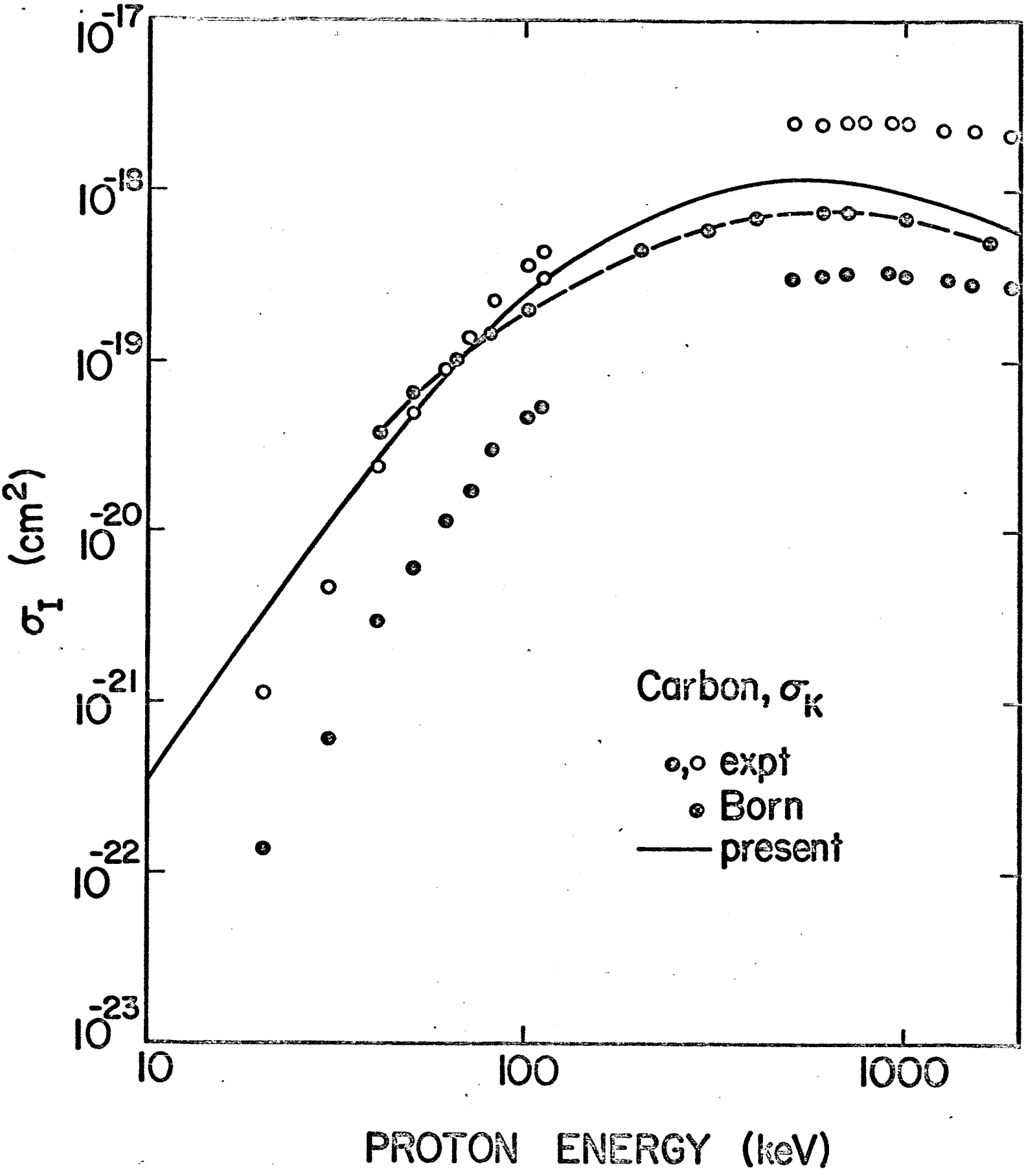

GARCIA Phys. Rev Fig 2

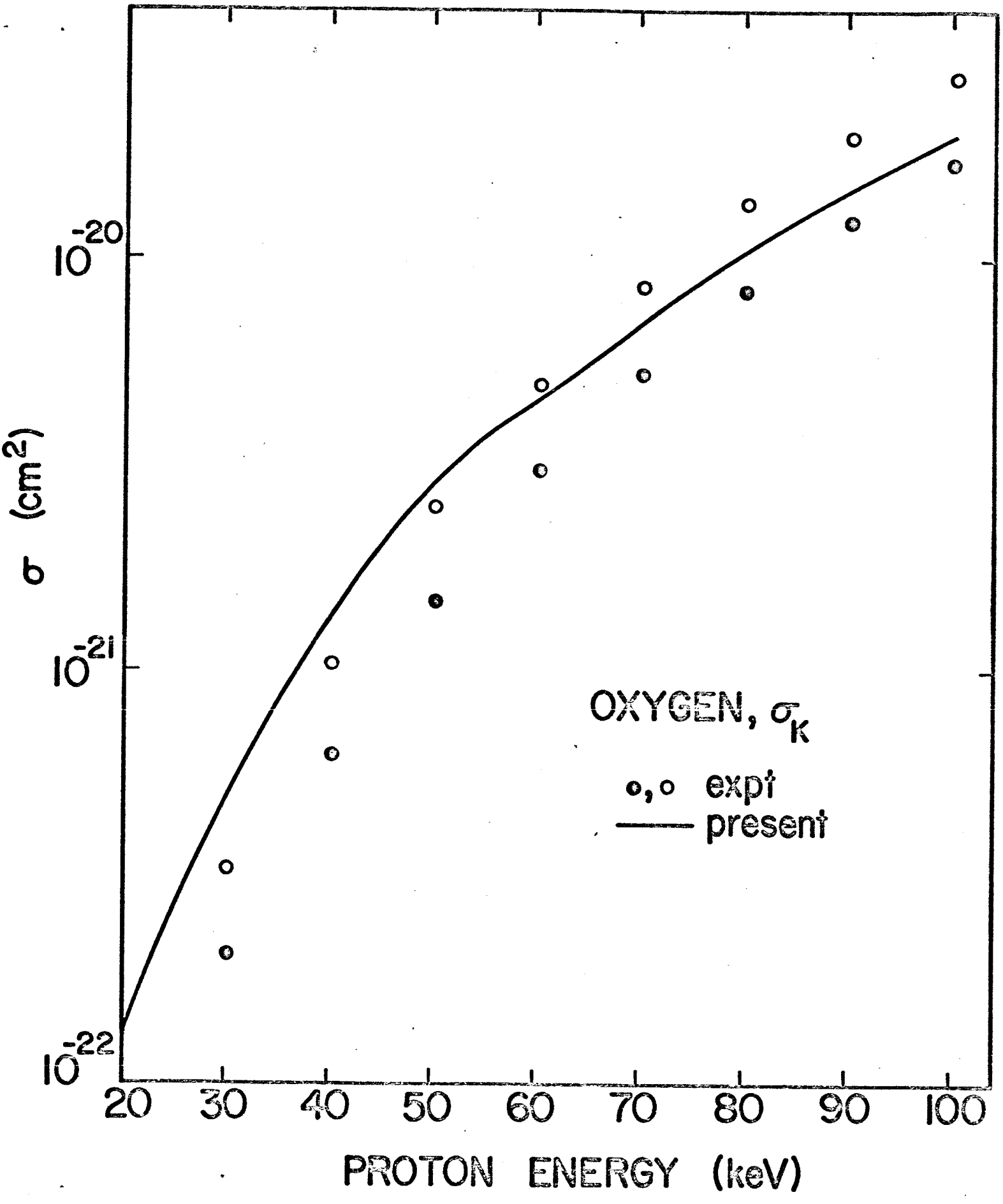

GARCIA Phys. Rev. Fig 3

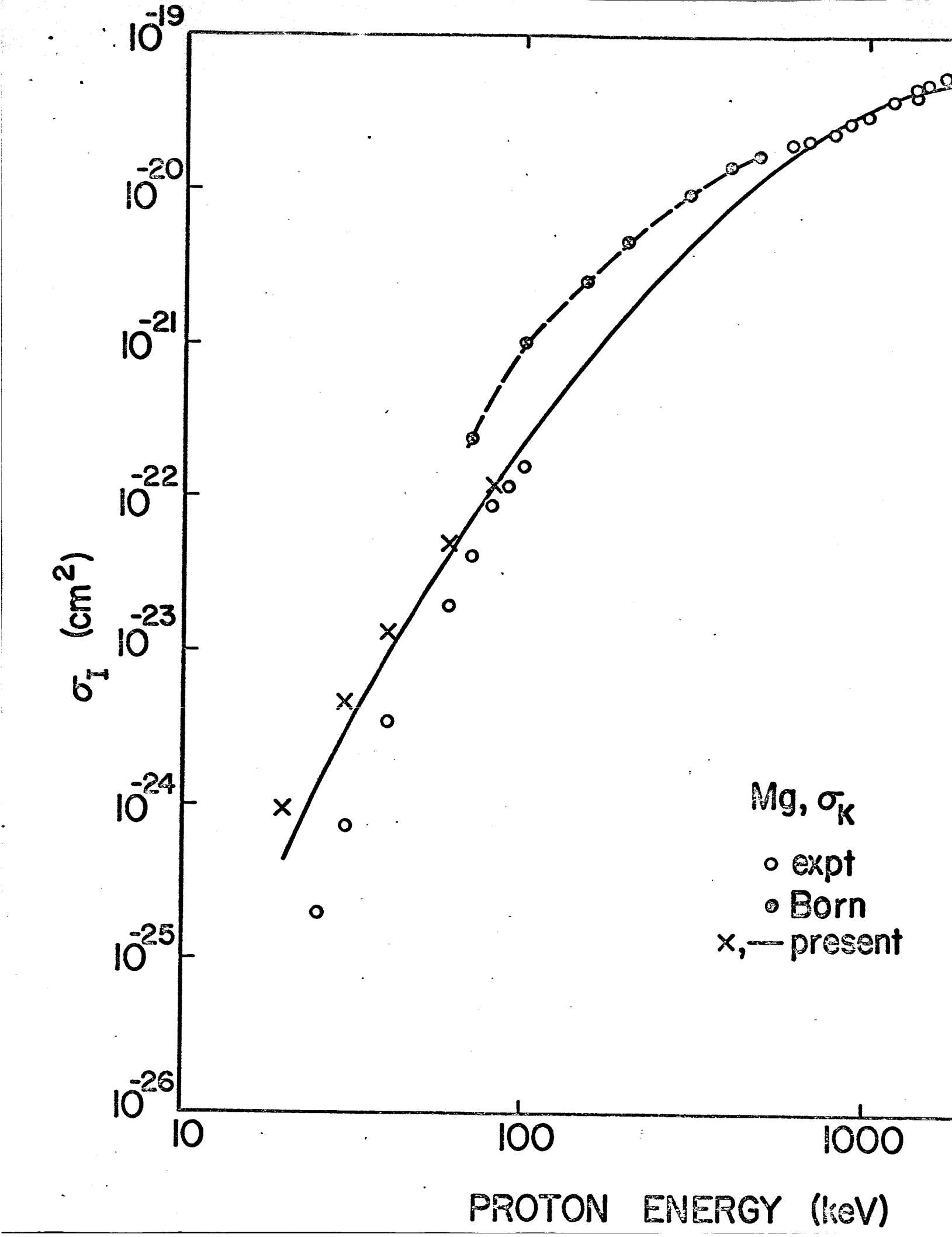
10^{-19}
10^{-20}
10^{-21}
10^{-22}
10^{-23}
10^{-24}
10^{-25}
10^{-26}
σ_I (cm^2)
10
100
1000
PROTON ENERGY (keV)
Mg, σ_K
o expt
o Born
x,— present

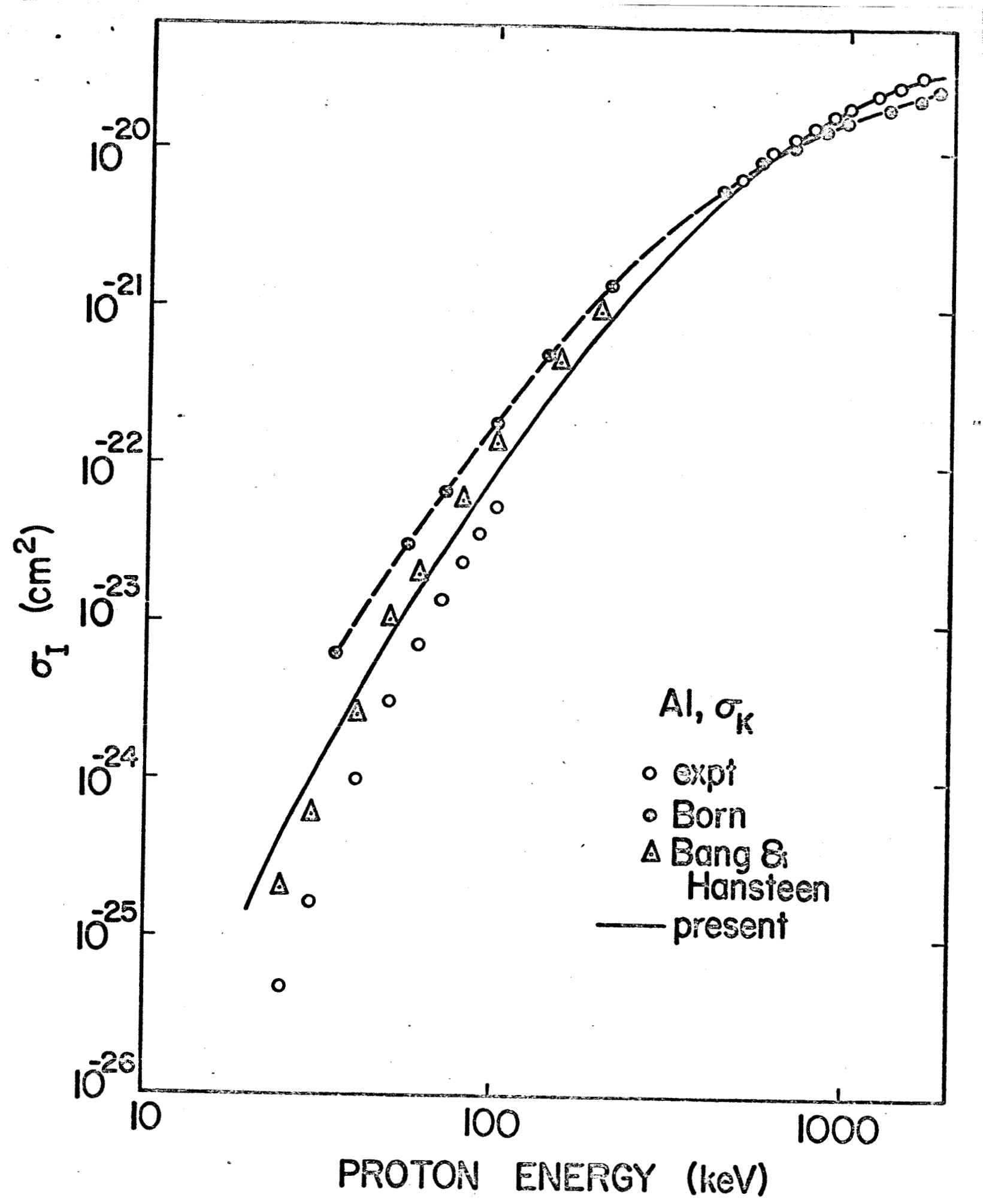

GARCIA Phys. Rev. Fig 5

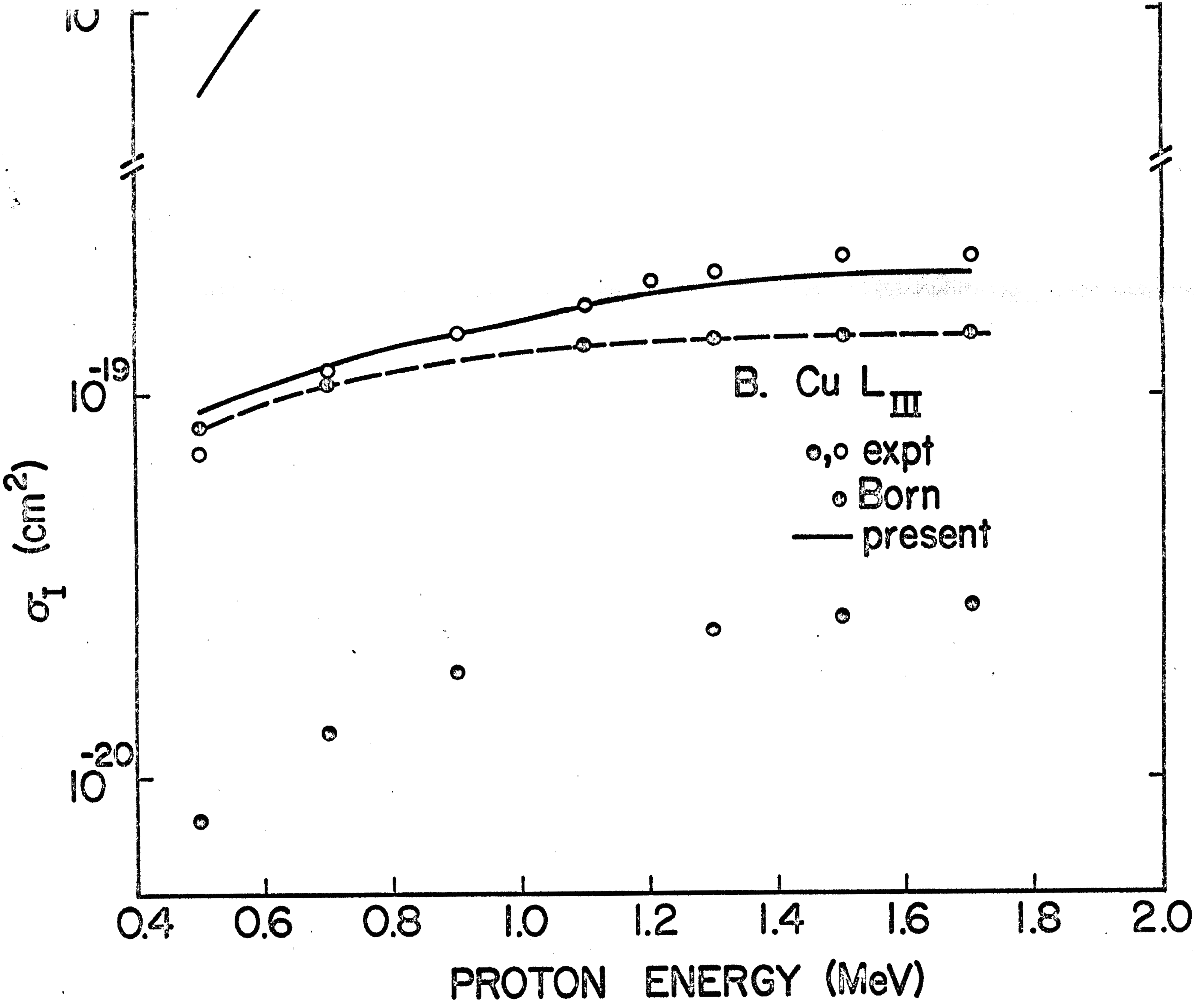

Garcia Phys Rev Fig. 6

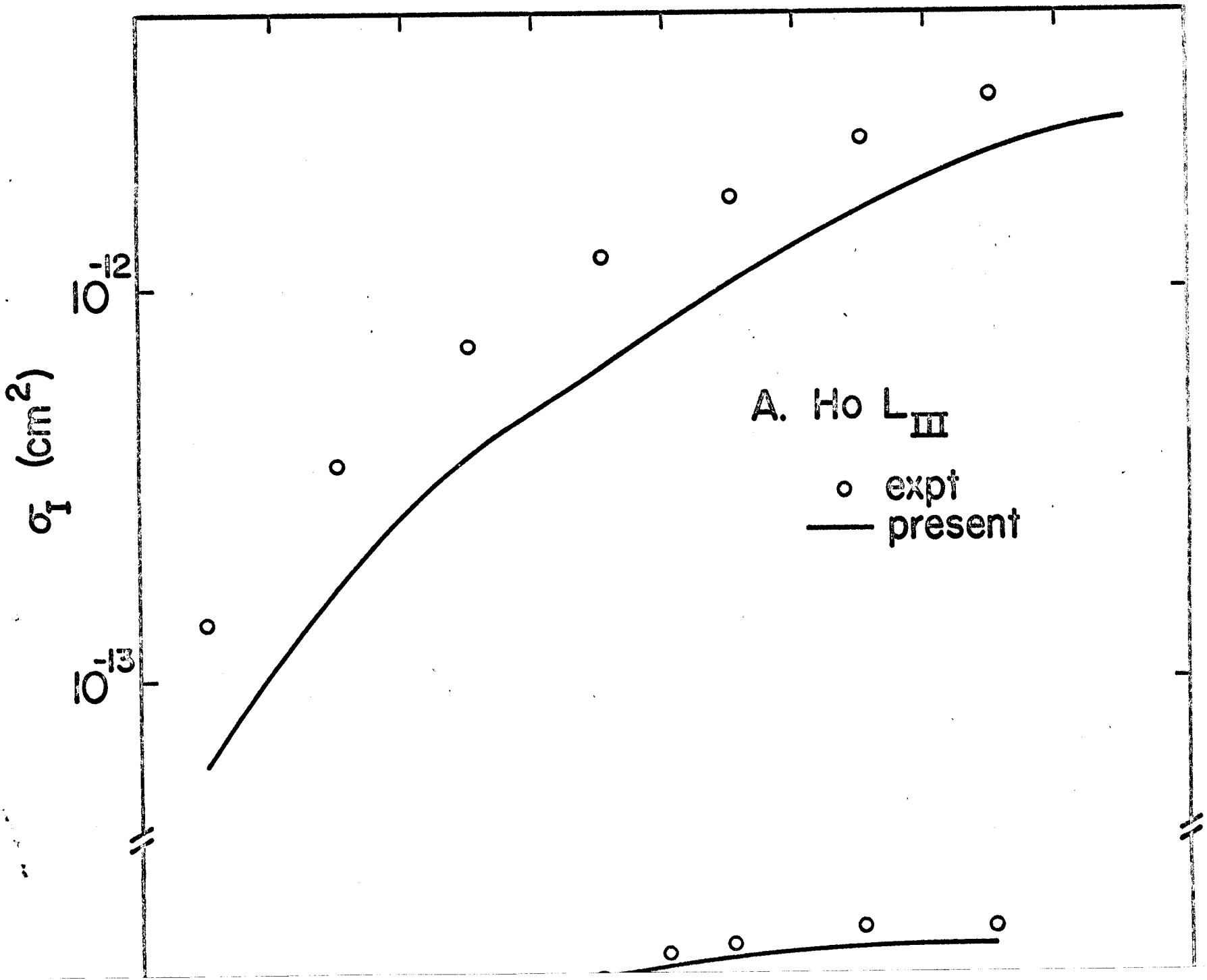
10^{-12}
10^{-13}
σ_I (cm^2)
A. Ho L_{III}
expt
present

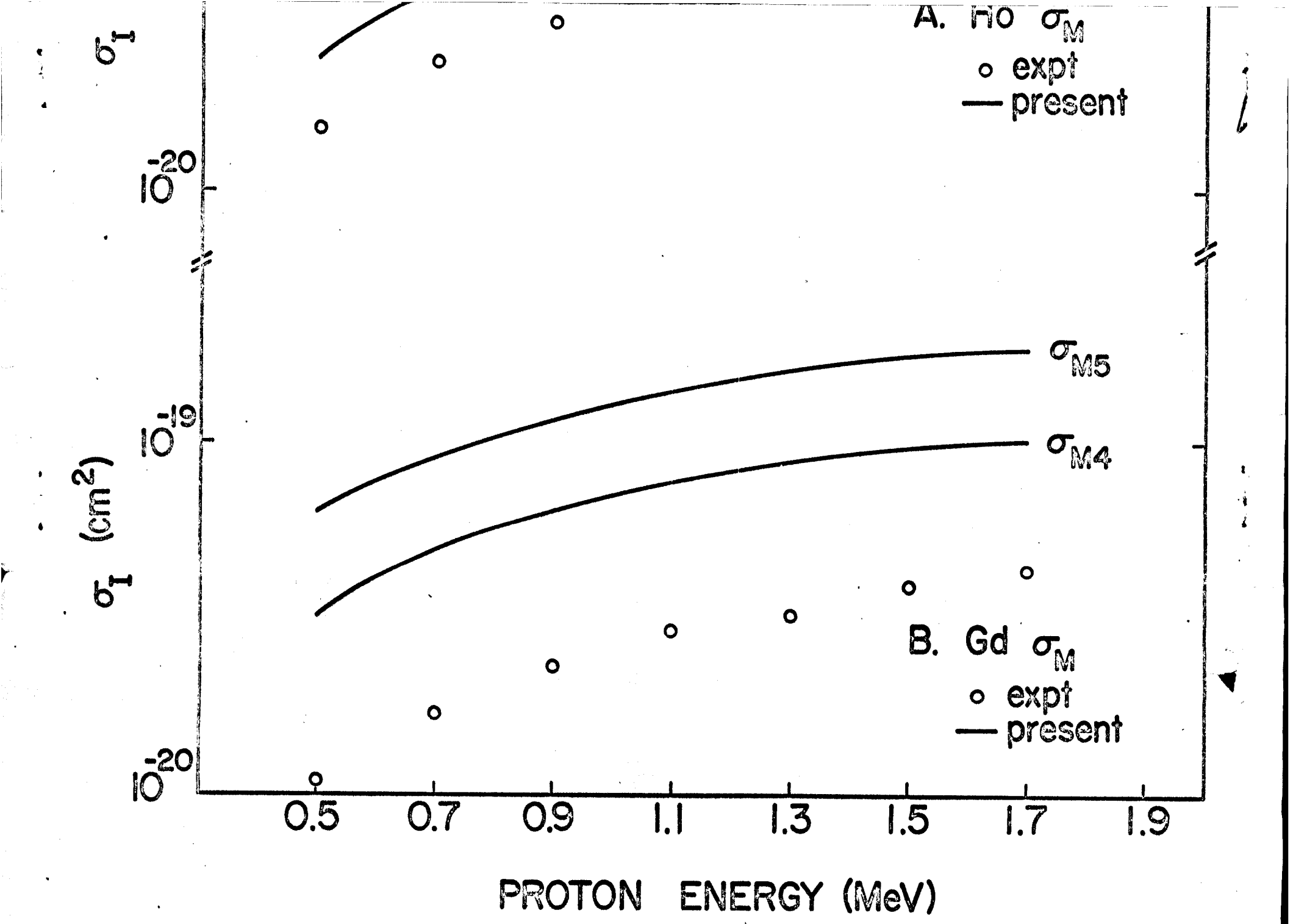

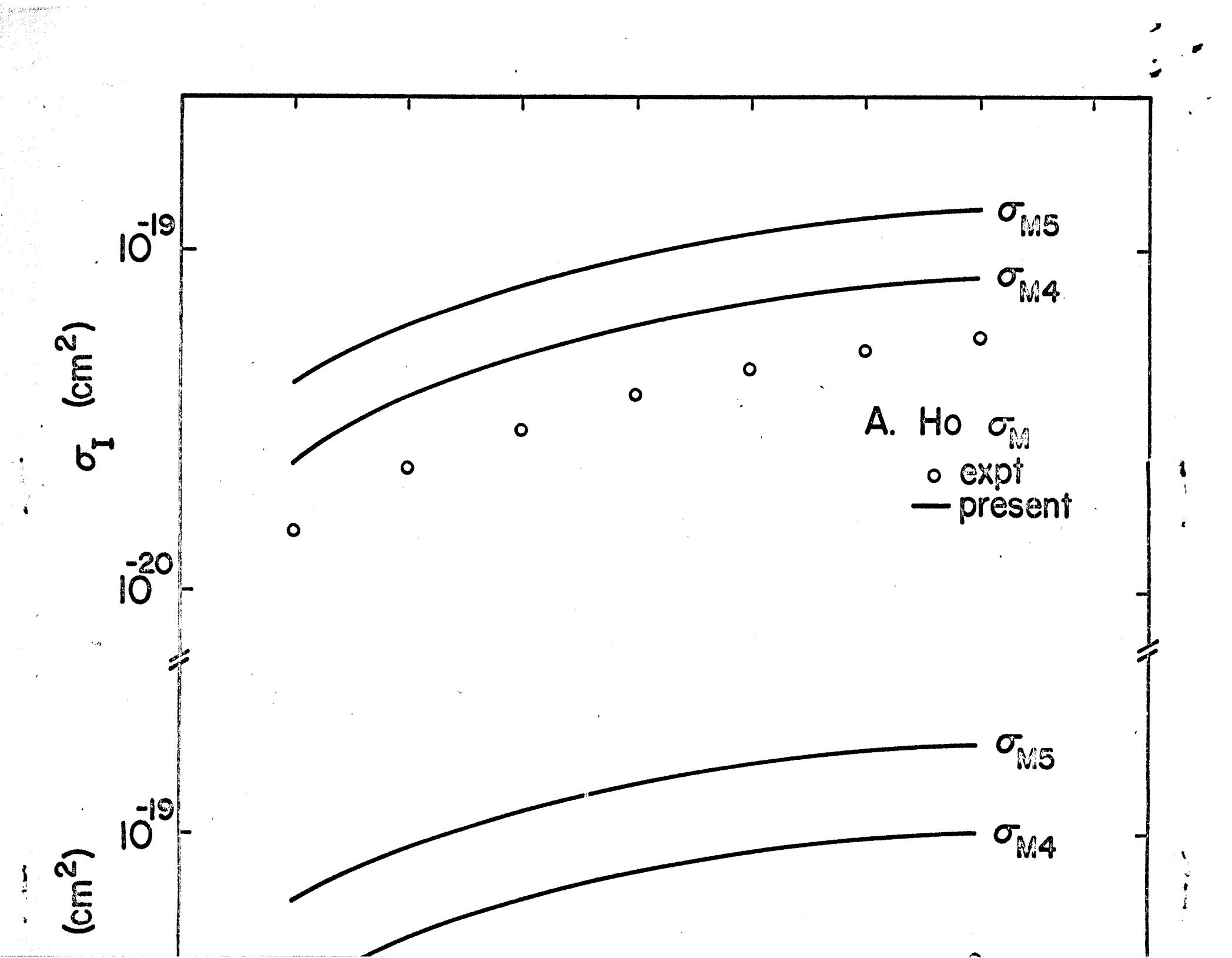
σ_{M5}
σ_{M4}
A. Ho σ_M
o expt
— present
10^{-19}
10^{-20}
σ_I (cm^2)
σ_{M5}
σ_{M4}
10^{-19}
(cm^2)